

MODELING AND MEASUREMENTS OF SPIN DEPOLARIZATION

N. Carmignani, F. Ewald, L. Farvacque, B. Nash, P. Raimondi, ESRF, Grenoble, France

Abstract

An electron bunch in a storage ring becomes spin polarized due to the Sokolov-Ternov effect. The beam may then be depolarized by applying a horizontal magnetic field oscillating in resonance with the spin tune. This technique has been used to measure the electron energy at numerous synchrotrons. In this paper, we report on modeling and measurements of the polarization and depolarization process at the ESRF. We report the results of a Matlab based parallelized spin tracking code that we developed for these studies. We show the change in depolarization resulting as different physical effects are added to the model.

SPIN DYNAMICS

Each electron in a beam has a spin which may be represented as a point on a sphere \vec{S}_j . The polarization of the beam may then be defined as $\vec{P} = \frac{1}{N} \sum_j \vec{S}_j$, where N is the number of particles.

An electron beam becomes spontaneously polarized due to the Sokolov-Ternov effect in which spin flips induced by synchrotron radiation cause preferentially polarization in the direction opposite to the magnetic field of the dipole magnets [1].

As the electron passes through magnetic fields it receives transverse orbital kicks $\theta_{x,y,orbit} = (-\Delta y', \Delta x')^1$. The corresponding spin kick is then given by

$$\Delta\theta_{x,y,sp} = a\gamma\Delta\theta_{x,y,orbit} \quad (1)$$

where $a = (g - 2)/2 = 0.0011596$ with g the anomalous magnetic moment of the electron and γ is the relativistic energy factor. Thus the net result of the dipoles in one revolution around the ring is to rotate the spin vector about the y axis by the spin tune $\nu_{sp} = a\gamma$.

After equilibration, the spins in the ring will continue to precess at the spin tune frequency. We now consider adding a vertical oscillating magnetic kicker to the ring with the goal of depolarization. The vertical orbit kick is given by

$$\theta_{orbit} = \theta_k \cos(\omega_k t) \quad (2)$$

Then, using Eqn (1), we get the kick to the spin by an angle

$$\theta_{x,sp} = a\gamma\theta_k \cos(\omega_k t) \quad (3)$$

Here we may also define the tune of the kicker, by dividing the kicker frequency by the revolution frequency

$$\nu_k = \frac{\omega_k}{\omega_0} \quad (4)$$

¹ Note that we use the coordinates (x, y, z) where y is vertical, z is the direction of the particle orbit, and x points out of the ring.

The polarization reduces the scattering cross section of the electrons and increases the Touschek lifetime. This latter can be calculated via:

$$\frac{1}{\tau_t(|\vec{P}|)} = \frac{1}{\tau_t(0)} + Q|\vec{P}|^2 \quad Q < 0 \quad (5)$$

where the expression for Q can be found in reference [2] and depends on the lattice functions and momentum acceptance. The polarization evolves with time as:

$$\vec{P}(t) = \vec{P}_{max} \left(1 - e^{-\frac{t}{\tau_p}}\right) \quad (6)$$

with τ_p being the polarization time.

POLARIZATION AND DEPOLARIZATION AT THE ESRF

For the ESRF, the theoretical polarization time is $\tau_p = 15.6$ min (using equation 4 in section 2.7.7 in reference [1]). If we assume the Sokolov-Ternov maximum polarization of $P_{ST} = 0.9238$ and a constant momentum acceptance of 2.5%, we obtain a lifetime increase of 15.1%.

The polarization at the ESRF was measured using the Touschek lifetime, as given by equation (5) and (6). The result is shown in figure 1. Fitting the curve, we obtain $\tau_p = 15.9 \pm 0.6$ min and $\Delta\tau_t/\tau_t = 0.150 \pm 0.005$ [3]. These values are very close to the theoretical ones, which is an indication that the final polarization P_{max} is close to the Sokolov-Ternov value.

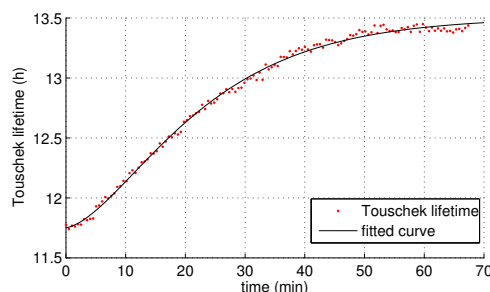


Figure 1: Polarization measurement at the ESRF via Touschek lifetime. The Touschek lifetime has been normalized to account for current and bunch length change and the measured vacuum lifetime has been subtracted.

The method of resonant spin depolarization allows a precise measurement of electron beam energy [4] [5]. We tried to apply this technique at the ESRF, however, the observed frequency range leading to depolarization was orders of magnitudes wider (~ 20 kHz) than expected (few Hz), see figure 2. This result and the difficulty of defining the correct experimental parameters motivated a more careful analysis of the depolarization process. A code based on AT² was written

² ATfasting function [6] was used for tracking speed.

for this study. We call the code FESTA (Fast Electron Spin Tracking based on AT). Many different effects were included as we will now describe.

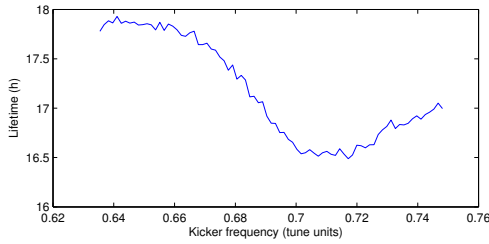


Figure 2: ESRF measurement of beam depolarization as the shaker frequency is swept across the spin resonance. Kick strength: 0.05 μ rad; excitation time: 10 s; step size: 500 Hz.

DEPOLARIZATION MODELING

FESTA tracks the spin of many particles as they propagate in the storage ring lattice while being excited by an oscillating magnetic field (kicker). The output of the code is the polarization of the electron beam after N turns. For accurate modeling, we distinguish the following cases in which more phenomena are added to the spin dynamics

- Case 0: All electrons have the same energy and precess about the vertical axis at $\nu_{sp0} = a\gamma_0$.
- Case 1: Energy spread is added.
- Case 2: Synchrotron oscillations are added.
- Case 3: Radiation damping and quantum diffusion effects are added.
- Case 4: The influence of kicker induced orbit oscillations in the quadrupoles is added.

Case 0: Fixed Energy

Here, we expect to be able to depolarize only within a very narrow width of the spin tune. The kicker will depolarize the beam when it imparts a total angle of $\pi/2$. This leads to a depolarization in N_{d0} turns, where

$$N_{d0} = \frac{\pi^2}{4\theta_k \nu_{sp0}} \quad (7)$$

For the ESRF spin tune of 13.707 and a kick strength of 1μ rad, this gives depolarization in 180,000 turns. In the later cases with more complex dynamics, it is expected that the depolarization would generally take longer.

Case 1: Energy Spread

Next, we add energy spread σ_δ which causes a spread in spin tune of $\sigma_{\nu_{sp}} = \nu_{sp0}\sigma_\delta$. In this case one gets depolarization in a broad range covering the spread in spin tune, which is directly linked to the spread in electron energy.

Case 2: Synchrotron Oscillations

When adding synchrotron oscillations, the depolarization resonance and its sidebands are found to become quite narrow again. This effect is analogous to motional narrowing in NMR [7]. The longitudinal component of the spin is seen to be modulated by the synchrotron oscillations as follows

$$S_z(t) = \sqrt{1 - S_y^2} \cos\left(\omega_0 \nu_{sp0} t + \frac{\nu_{sp0} \delta_0}{\nu_s} \sin(\omega_s t)\right) \quad (8)$$

where δ_0 is the amplitude of the energy oscillation of the given electron, ν_s is the synchrotron tune, S_y is the vertical spin, which is constant during the precession. We may now apply the identity

$$\cos(\omega_c t + B \sin \omega_m t) = \sum_{n=-\infty}^{\infty} J_n(B) \cos(\omega_c + n\omega_m)t \quad (9)$$

where we identify

$$\begin{aligned} \omega_c &= \omega_0 \nu_{sp0} \\ \omega_m &= \omega_s = \omega_0 \nu_s \\ B &= \frac{\omega_0 a \gamma_0 \delta_0}{\omega_s} = \frac{\nu_{sp0} \delta_0}{\nu_s} \end{aligned} \quad (10)$$

Using the identity in equation 9, the Fourier transform of equation 8 can easily be performed to obtain the spectrum of resonances. Figure 3 shows this spectrum (narrow lines) for two different lattices: the ESRF (light blue) and the Australian Synchrotron (green). As expected from equation 9 we find a sharp resonance at the spin tune with its synchrotron tune satellites, while $J_n(B)$ determines the envelope³. B may be simply interpreted as the number of sidebands inside the spin tune spread (replacing δ_0 with σ_δ) and therewith also defines the density of sidebands. B is also known in the literature as the spin tune modulation index [9]. The ESRF has a B -value of 2.68 and thus a denser sideband distribution than the AS ($B = 0.65$) where only a few, well spaced sidebands appear.

Case 3: Radiation Effects

To understand the effect of adding radiation, we analyzed the spectrum of the spin motion. We took an FFT of equation 8 with damping and diffusion added where AT tracking was used to find $\delta(t)$ with ESRF and AS lattices. The results in figure 3 show a dramatic degradation of the ESRF spectrum when radiation is added. The spectrum of AS is broadened but much less so. A shift in the spectrum is also seen when radiation is added, which should be investigated further.

Running FESTA including these radiation effects we obtain the beam polarization as shown in figure 4. While for the AS the sidebands are very narrow and perfectly distinct, this is not at all the case for the ESRF: there is an overall possibility for depolarization for whatever kicker tune will be applied within the width of the tune spread.

³ See [8] for experimental verification of this point for the case of deuterons. In that case, the synchrotron oscillations could be turned on or off via the RF cavity, and the resonance width broadening could be observed.

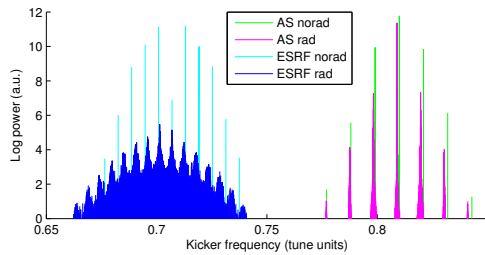


Figure 3: Spectra with and without radiation effects for ESRF and AS parameters.

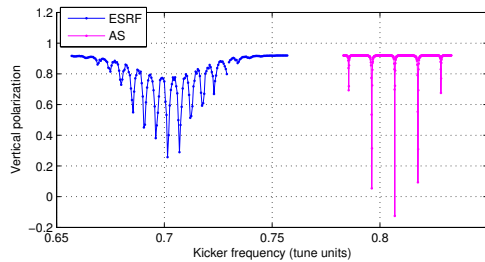


Figure 4: FESTA result for depolarization including energy spread, synchrotron oscillations, and radiation damping and quantum diffusion. The kicker strength is 25 μ rad and 100 particles were tracked for 1 million turns.

Case 4: Effects of Quadrupoles

Finally, we need to consider that orbital offsets in the quadrupoles will generate additional spin rotation. We can parametrize this rotation R with three angles $\vec{\Theta} = (\theta_x, \theta_y, \theta_z)$. Using element by element orbit and spin tracking for one turn, we compute a 3×6 matrix \mathcal{O} which we call the Orbit Angle Matrix (OAM). Let \vec{z}_n be the phase space coordinates on the n^{th} turn. We may compute the three angles $\vec{\Theta}_n = \mathcal{O}\vec{z}_n$. The rotation matrix for the spin is then given by

$$R_n = R_{x,\theta_{x,n}} R_{y,\theta_{y,n}} R_{z,\theta_{z,n}} R_{y,2\pi\nu_{sp0}} \quad (11)$$

where we have added the large rotation via the spin tune at the end. The OAM may be seen as a generalization of the spin response function [10] [11]. It depends on the position in the lattice. In figure 5 four components of the ESRF OAM as a function of the position in the lattice are shown.

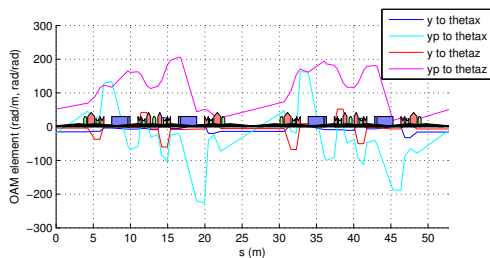


Figure 5: Orbit angle matrix for ESRF.

Figure 6 shows the influence of the quadrupoles on the depolarization at the ESRF. In contrast to the AS the res-

onance and its sidebands become quasi indistinguishable, and complete depolarization can be achieved in the whole range of the tune spread. This simulation result corresponds to our experimental findings at the ESRF.

In both cases, we find that the depolarization rate increases when approaching the vertical tune resonance, that are 0.61 ($1 - 0.39$) for the ESRF and 0.784 ($1 - 0.216$) for the AS.

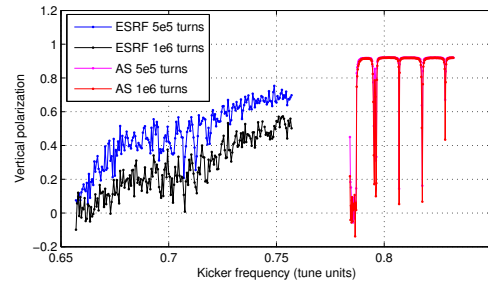


Figure 6: Same as figure 4, including the OAM, that amplifies the effect of the kicker. The kicker strengths are reduced to 1 μ rad for the ESRF and to 10 μ rad for the AS, while the number of turns is kept the same.

The output of the simulation, as shown in figure 6, helps to understand the experimental results found at the ESRF. The data in figure 2 shows the cumulative effect of depolarization while scanning slowly through the kicker tune (without waiting for repolarization after each excitation). So, experimentally the measurement represents the integral of the simulation data shown in figure 6 as a function of the kicker tune. Since all the sidebands of the spin tune resonance overlap and the resonances have no contrast, they can't be detected experimentally. In the same way, the sharp and well distinct depolarization resonances found for the AS-case are in line with the clear experimental evidence of the resonances reported in [4].

CONCLUSION

We have studied spin depolarization dynamics in an effort to model a broad depolarization region found in ESRF measurements. We have seen this broadening in simulation and its dependence on one key parameter: $B = \nu_{sp0}\sigma_\delta/\nu_s$. The parameter B is seen to control the envelope of the spectrum of the main resonance and synchrotron sidebands. It may also be seen simply as the number of sidebands inside the spin tune spread. We observe that many electron storage rings that were able to detect the sharp resonance and its side bands have a $B < 1.5$ (including LEP with $B = 1.3$), while the ESRF has a rather high value $B = 2.68$.

More benchmarking and development of the FESTA code is foreseen with comparison to measurements of spin polarization at other storage rings. This should give confidence in the code and shed more light on the ideal conditions for successful spin resonance detection.

We would like to acknowledge discussions with N. Monseu, D. Barber, T. Ziman, M. Clusel. We thank E. Tan, K. Wootton and M. Boland for providing the AS lattice.

REFERENCES

- [1] A. W. Chao et al. "Handbook of accelerator physics and engineering." World Scientific, 1999.
- [2] T.-Y. Lee et al., "Simple determination of Touschek and beam-gas scattering lifetimes from a measured beam lifetime", Nuclear Instruments and Methods in Physics Research A 554 (2005).
- [3] N. Carmignani, PhD thesis, Università di Pisa (2014).
- [4] K. P. Wootton, et al. "Storage ring lattice calibration using resonant spin depolarization." Physical Review Special Topics-Accelerators and Beams 16.7 (2013): 074001.
- [5] L. Arnaudon, et al. "Accurate determination of the LEP beam energy by resonant depolarization." Zeitschrift fur Physik C Particles and Fields 66.1-2 (1995): 45-62.
- [6] B. Nash et al., "New Functionality For Beam Dynamics in Accelerator Toolbox (AT)" IPAC 2015, MOPWA014.
- [7] A. Abragam, "The Principles of Nuclear Magnetism", Oxford University Press (1961).
- [8] V.S. Morozov et al., "Narrow Spin Resonance Width and Spin Flip with an rf-Bunched Deuteron Beam", PRL 103, 144801 (2009).
- [9] J. Buon, "A Stochastic Model of Depolarization Enhancement due to Large Energy Spread in Electron Storage Rings", LAL-RT 88-13 (1988).
- [10] P. Kuske, T. Mayer, "Set Up for Beam Energy Measurements at BESSY II", Proceedings of EPAC 1996.
- [11] H. Xu et al., "Equipment for Electron Beam Energy Calibration in HLS", Proceedings of EPAC 2008.